



HAL
open science

Interactions between high temperature deformation and crystallization in zirconium based bulk metallic glasses

Sébastien Gravier, Jean-Jacques Blandin, Patricia Donnadiou

► **To cite this version:**

Sébastien Gravier, Jean-Jacques Blandin, Patricia Donnadiou. Interactions between high temperature deformation and crystallization in zirconium based bulk metallic glasses. *Philosophical Magazine*, 2008, 88 (16), pp.2357-2372. 10.1080/14786430802192112 . hal-00513905

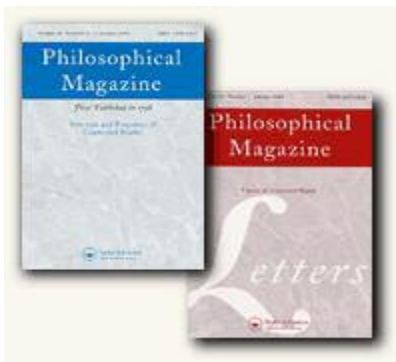
HAL Id: hal-00513905

<https://hal.science/hal-00513905>

Submitted on 1 Sep 2010

HAL is a multi-disciplinary open access archive for the deposit and dissemination of scientific research documents, whether they are published or not. The documents may come from teaching and research institutions in France or abroad, or from public or private research centers.

L'archive ouverte pluridisciplinaire **HAL**, est destinée au dépôt et à la diffusion de documents scientifiques de niveau recherche, publiés ou non, émanant des établissements d'enseignement et de recherche français ou étrangers, des laboratoires publics ou privés.



Interactions between high temperature deformation and crystallization in zirconium based bulk metallic glasses

Journal:	<i>Philosophical Magazine & Philosophical Magazine Letters</i>
Manuscript ID:	TPHM-07-Mar-0084.R1
Journal Selection:	Philosophical Magazine
Date Submitted by the Author:	30-Jan-2008
Complete List of Authors:	Gravier, Sébastien; INP Grenoble, SIMAP Blandin, Jean-Jacques; INP Grenoble, SIMAP Donnadieu, Patricia; INP Grenoble, SIMAP
Keywords:	amorphous metals, crystallization, nanocrystals, viscosity
Keywords (user supplied):	high temperature deformation



Interactions between high temperature deformation and crystallization in zirconium based bulk metallic glasses

S. GRAVIER, J.J. BLANDIN, P. DONNADIEU

Science et Ingénierie des Matériaux et des Procédés (SIMAP)
INP Grenoble / CNRS / UJF
38402 Saint-Martin d'Hères Cedex, France

Abstract

High temperature deformation of a ZrTiCuNiBe bulk metallic glass (BMG) is investigated by compression tests in the supercooled liquid region. When temperature is decreased or strain rate is increased, the amorphous alloy exhibits the usual Newtonian – non Newtonian behavior transition. Owing to appropriate heat treatments, partially crystallized alloys are produced, the associated microstructures are characterized and the volume fractions of crystal are measured. The interaction between high temperature deformation and crystallization is investigated by appropriate mechanical tests. According to the mechanical measurements, partial crystallization is responsible for an important increase of the flow stress and a promotion of the non-Newtonian behaviour. The deformation does not change significantly the volume fraction of crystal, the crystal composition neither the size. The flow stress increase with crystallization is analyzed under different hypotheses. It comes out that the flow stress increase can not be interpreted through a composition change in the residual amorphous matrix neither by the reinforcement due to hard crystallites nor by connections between crystals. It finally seems that the effect is rather due to the nanometric size of the crystals.

Keywords

Bulk metallic glass; high temperature deformation; crystallization; viscosity; nanocrystal

1. Introduction

In the last decade, bulk metallic glasses (BMG) have been extensively studied since it is now possible to produce them with relatively large dimensions. In particular, the mechanical properties at room temperature of BMG have focused interest since these materials generally exhibit high value of the fracture stress with a particularly large elastic domain [1]. BMG also exhibit a superplastic-like behavior in the supercooled liquid region (SLR) [2,3]. It has been shown that the homogeneous viscous flow behavior of BMGs in SLR can be Newtonian or non-Newtonian, depending on testing temperature and strain rate [4,5]. The Newtonian flow (i.e. flow stress linearly dependent on the applied strain rate or viscosity independent on strain rate) is typically obtained at high temperature and low strain rates. The transition from Newtonian to non-Newtonian flow behavior when the strain rate is increased or when the temperature is reduced, has been attributed to stress-induced formation of defects in the bulk glassy alloy [6], which limits the increase of the flow stress.

However, since their elaboration requires relatively rapid solidification from the melt, BMG structures are out of equilibrium with respect to crystalline state. While reheated into the SLR, crystallization and/or transformation into other metastable phases may occur, leading to changes of the mechanical behavior at ambient as well as high temperatures. The effect of crystallization on the fracture stress at room temperature depends mainly on the volume fraction and the size of the crystals. When the crystallite size is no more than few tens of nanometers, the fracture stress often increases slightly until a critical content in crystallites and then falls significantly [7-9]. At high temperature, the effect of nanocrystallization on deformation remains poorly analyzed. On the Vit1 alloy ($Zr_{41.2}Ti_{13.8}Cu_{12.5}Ni_{10}Be_{22.5}$, at. %), Waniuk *et al.* [10] carried out bending tests in the SLR and detected after an incubation time, a huge increase of the viscosity. This hardening was attributed to several causes: the formation of nanocrystals in the viscous matrix but also a phase decomposition which may occur in this alloy before crystallization or a change in the composition of the residual glass as far as crystallization occurs. Similar reinforcement due to nanocrystallization were also observed on different BMGs bases [11, 12].

Deleted: documented

Deleted: Kim *et al.* [11] found s

Deleted: results during tensile tests of another zirconium based BMG

Deleted: .

The coupling between deformation and crystallization was also partially studied recently and some studies have shown that high temperature deformation can accelerate crystallization kinetics [13,14, 15]: for instance, after tensile tests on a Zr based BMG, nanocrystals were observed in the sample gauge length whereas the alloy was still amorphous in the non deformed region. Conversely, in the case of the formation of quasicrystals, it was observed that deformation in the non Newtonian regime could slow down the quasi-crystallization kinetics while the deformation in the Newtonian regime had no detectable influence [16]. Quasi-crystallization requiring an icosahedral local structure in the glass, if viscous flow strongly increases structural disorder, this may hinder quasi-crystallization.

The aim of this paper is thus to get experimental information about the influence of the crystallization on the high temperature deformation and more precisely to investigate the interactions between high temperature deformation and crystallization in the Vit1 BMG.

2. Experimental procedure

The investigated alloy was supplied by Howmet Corp. (USA). Differential scanning calorimetry (DSC) at a heating rate of 10 K/min. was used to determine the characteristic temperatures and to get information about the crystallization energies. From DSC measurements, a temperature of 628 K was found for the onset of the glass transition temperature T_g^{on} in agreement with previously published data [10]. High temperature deformation was studied by compression tests in air. For the compression experiments, cylindrical samples of 3 mm in

1
2 diameter and 5 mm in height were machined from a plate of about 3 mm thickness. The samples
3 were heated to the testing temperatures at a heating rate of 20 K/min and held at the testing
4 temperature for about 300 s to homogenize temperature before starting compression. During
5 testing, the temperature is stabilized to ± 1 K. A thin superficial oxidized layer appears during
6 testing but to thin to affect the macroscopic behavior. The temperature range of interest was
7 between 623 K and 683 K. In this range, the glass was expected to be fully relaxed when
8 deformation started. Indeed, structural relaxation has been studied in detail for the Vit1 alloy
9 [6,17,18]: at 643 K, a relaxation time of about 20 s has been reported whereas a relaxation time
10 close to 300 s is expected only for temperatures close to 623 K. X-Ray Diffraction (XRD) with
11 Cu K α radiation was used to investigate the microstructure evolution after static and dynamic
12 annealing at the given temperatures. Transmission electron microscopy (TEM) was also carried
13 out, the observations being performed at 300kV in a JEOL 3010 microscope. An ion beam
14 milling method was used to prepare the thin foils.

15 3. Mechanical behaviours in the SLR

16
17 In order to get information about the rheology of the glass, strain rate jump tests were
18 carried out for temperatures between 623 K (i.e. $T_g^{on} - 5$ K) and 683 K (i.e. $T_g^{on} + 55$ K) and
19 using the experimental data from the strain rate increase tests, the apparent viscosity η_{app} was
20 calculated and the evolution of η_{app} with the applied strain rate is shown in figure 1 for the
21 investigated temperatures. Depending on the temperature, the strain rate interval was more or
22 less extended in order to avoid crystallization during the tests. To check that, a strain rate applied
23 during the first jumps was repeated at the end of each test and the resulting stress was compared
24 to the value initially obtained. These comparisons confirmed that in the studied experimental
25 conditions, no significant hardening occurred during the strain rate jump tests.

26 [Insert figure 1 here: Viscosity vs. strain rate in compression for the
27 amorphous alloy at various temperatures]
28

29 For the investigated conditions, the apparent viscosity varies roughly from 10^9 Pa.s to
30 10^{12} Pa.s. Since the glass is expected to be fully relaxed when the test starts, the Newtonian
31 viscosity which is measured corresponds to an equilibrium viscosity. For the same glass
32 deformed in compression, a Newtonian viscosity close to 4×10^{10} Pa.s was reported at 643 K [6]
33 which is in good agreement with the value of about 4×10^{10} Pa.s measured in the present work at
34 646 K and for strain rates slightly lower than 5×10^{-4} s $^{-1}$. Apparent viscosities equal
35 approximately to 3×10^{10} Pa.s for bending tests at 643 K in the first 20 minutes of testing were
36 also reported for the same alloy [10].

37 As usually obtained during high temperature deformation of bulk metallic glasses, a
38 Newtonian domain is detected for high temperature and/or low strain rates. At a given
39 temperature, the viscosity tends to decrease for high strain rates, the mechanical behavior
40 becoming then non Newtonian. In the studied experimental domain, the critical strain rates
41 corresponding to the transition from Newtonian to non-Newtonian regimes at a given
42 temperature are in good agreement with previously published results [6]. For the lowest
43 temperatures ($T \leq 633$ K), it becomes more difficult to obtain direct experimental measurements
44 of the Newtonian viscosity. In such conditions, it is fruitful to use a master curve in order to get
45 an estimation of the Newtonian viscosity as performed by Bletry et al. [19]. This extrapolation
46 confirms that the Newtonian viscosity is very sensitive to temperature since under the
47 assumption of an Arrhenius law $\eta_N = \eta_0 \exp(Q_{app}/kT)$, a value of an apparent activation energy
48 Q_{app} of about 4.5 eV can be measured, in agreement with previously reported values of Q_{app} for
49 Zr-based BMG deformed in the SLR [5,20,21].
50
51
52
53
54
55
56
57
58
59
60

1
2 From these data, two temperatures were selected: 646 K and 683 K. This choice was
3 motivated by the ability to have information about the thermal stability of the Vit1 during the
4 mechanical tests. Figure 2a displays the evolution of the flow stress with strain for the following
5 rates ($1.5 \times 10^{-4} \text{ s}^{-1}$, $2 \times 10^{-4} \text{ s}^{-1}$ and $3 \times 10^{-4} \text{ s}^{-1}$) at 646 K. For all the applied strain rates, at least two
6 domains can be detected for all curves: a first region in which the stress is roughly constant
7 followed by a region where the stress significantly increases. In the first region (up to a strain of
8 about 0.2), a quasi-Newtonian behavior is measured, in agreement with the results coming from
9 the strain rate jump tests (see figure 1). The situation is more unusual for larger strains. For a
10 strain close to 0.5, similar flow stresses are obtained for the three investigated strain rates and for
11 larger strains ($\epsilon > 0.5$), apparent negative strain rate sensitivity parameters are measured. For
12 instance, at $\epsilon = 1.0$, the flow stress is reduced from 130 MPa to 70 MPa when the strain rate is
13 multiplied by a factor 2. Since hardening is attributed to crystallization which may occur at this
14 temperature, this result confirms the idea that care must be taken in the choice of the conditions
15 of forming of BMG in the SLR if partial crystallization cannot be avoided.

16 [Insert figure 2a here: Flow stress vs. strain at 646 K for various strain
17 rates]

18 [Insert figure 2b here: Apparent viscosity vs. time at 646 K for various
19 strain rates]

20 These data can be rationalized if curves (η, t) (with η the apparent viscosity) are drawn
21 instead of (σ, ϵ) (see Figure 2b). For the three investigated strain rates, similar curves are
22 observed. Up to an incubation time t_{inc} of about 1800 s (t_{inc} appears independent on the applied
23 strain rate), viscosities close to $4 \times 10^{10} \text{ Pa.s}$ are measured. For $t > t_{\text{inc}}$ (keeping in mind that the
24 compression tests start after 300 s of temperature stabilization), the viscosities increase similarly
25 whatever the strain rate is. The mechanical test at the highest strain rate ($3 \times 10^{-4} \text{ s}^{-1}$) had to be
26 stopped after a total annealing time of 5000 s due to maximum load considerations. These results
27 are in agreement with Waniuk et al. [10], who reported also apparent viscosities equal
28 approximately to $3 \times 10^{10} \text{ Pa.s}$ at 643 K in the first 20 minutes of testing followed by a huge
29 increase of viscosity. This increase in viscosity can be measured by a reinforcement factor R
30 defined as the ratio of the viscosity after a given time by the viscosity of the glass before
31 crystallization.

32 Figure 2-c shows the effect on the R factor of heat treatments at the same temperature
33 before compression when the glass is deformed at $1.5 \times 10^{-4} \text{ s}^{-1}$. It is worth noting that when the
34 strain rate is fixed, plotting an evolution against stress or against viscosity is similar. Two more
35 heat treatment time before compression were selected: 3600 s and 7200 s. In both cases, when
36 the glass is deformed, the R curve superposes with the one corresponding to the alloy deformed
37 continuously. This behavior supports the idea that deforming the sample does not modify
38 significantly mechanical properties and consequently suggests that crystallization is probably not
39 strongly affected by deformation.

40 [Insert figure 2c here: Reinforcement factor vs. time at 646 K and $1.5 \times 10^{-4} \text{ s}^{-1}$
41 for various incubation times at 646 K: 300 s, 3600 s and 7200 s]

42 Similar mechanical characterizations were carried out for compression tests at 683 K at a
43 strain rate of $5 \times 10^{-4} \text{ s}^{-1}$. Figure 3 shows the effect on R of the duration of the heat treatment
44 before compression. Compared to what was observed at 646 K, there is a relatively short steady
45 state before the increase of the flow stress. Two hardening domains (before and after about 2200
46 s) can be distinguished where the slopes are different. Hardening can be very important since a
47 value of $R \approx 300$ can be measured between 300 s and 3000 s. The curves in figure 3 confirms
48 that strain is not the parameter which controls the variation of the mechanical properties of the
49 alloy since various annealing times before deformation (300 s, 900 s 1500 s and 2050 s) were
50

performed without changing neither the reinforcement factor nor the change in the variation with time of this factor. In other words, the reinforcement factor after a given time appears to be controlled by the total time spent at 683 K and not by the strain level.

[Insert figure 3 here: Reinforcement factor vs. time at 683 K and $5 \times 10^{-4} \text{ s}^{-1}$ for various incubation times at 683 K: 300 s, 900 s, 1500 s and 2050 s]

4. Discussion

4.1. Crystallization at 683 K and 646 K

4.1.1. Nature and size of the crystallites. As previously mentioned, important strain hardening has been already reported in the case of BMG and particularly for the Vit1 alloy [10]. Such stress hardening was mainly attributed to crystallization and phase separation effects. To get information about the crystallization kinetics at the investigated temperatures, DSC analyses at a heating rate of 10 K/min. were carried out on the as cast sample and on two samples heat treated at 646 K for 1800 s (corresponding to the time for which strain hardening starts when the glass is deformed at this temperature) and 7200 s respectively. The resulting DSC curves are shown in figure 4a. In the amorphous state, three exothermic peaks respectively at 710 K, 729 K and 777 K are observed after the SLR. These peaks are associated to three distinct crystallization events, knowing that the first one can also include phase separation [22,23]. After the holding time of 1800 s at 646 K, the first crystallization peak has been shifted to a lower temperature and has also been reduced whereas after 7200 s the first peak has totally disappeared. One can note that despite some slight variations in characteristic temperatures of the two other peaks with the holding time at 646 K, the associated crystallization energies remains roughly unchanged. Similar analyses were carried out after treatments performed at 683 K and the results are shown in figure 4b for two durations of treatments: 1200 s and 3600 s. After 1200 s, the first crystallization peak has disappeared while the crystallization energies for the two other ones remain roughly unchanged. Finally, after 3600 s, only the third peak is present. A longer heat treatment at this temperature has no major effect on the third crystallization peak. These observations confirm the idea that the increase of viscosity which has been detected during compression tests is due to the microstructural changes in the Vit1 during isothermal annealing at 646 K and 683K, including phase separation and nanocrystallization.

[Insert figure 4a here: DSC curves at a heating rate of 10K/mn of the as cast sample and of samples annealed 1800 s and 7200 s at 646K]

[Insert figure 4b here: DSC curves at a heating rate of 10K/mn of the as cast sample and of samples annealed 1200 s and 3600 s at 683 K]

Figure 5ab display bright field TEM observations after isothermal treatment for 600 s and 2700 s at 683 K. After 600 s, dispersed crystals can already be observed with an average size of 30 nm (the particle size distribution appearing relatively narrow) whereas after a holding time of 2700 s, the number of crystals increases but without significant change of the average size. Figure 5b suggests that even after a holding time of 2700 s at 683 K, the crystal volume fraction is high but the alloy is not fully crystallized. Figure 5c displays a dark field TEM observation of a sample annealed 7200 s at 646 K, suggesting the presence of nanocrystals with a mean size less than 10 nm in the amorphous matrix. This size is in agreement with measurements carried out by Löffler et al. [23], who concluded that the size was constant up to about 6 hours of maintain at this temperature.

[Insert figure 5a here: Bright field TEM observations of a sample heat treated at 683 K for 600 s]

[Insert figure 5b here: Bright field TEM observations of a sample heat treated at 683 K for 2700 s]

[Insert figure 5c here: Dark Field TEM observation of a sample annealed 7200 s at 646 K]

Figure 6 shows the variations of the XRD profiles with the isothermal holding time at 683 K. After 600 s, some small peaks can be detected suggesting that crystallization process has started, which is in agreement with the TEM observation (figure 5.a) and with the hardening observed during the compression tests carried out at this temperature. After 1200 s, crystallization is more obvious since three significant peaks can be identified. These peaks are attributed to an icosahedral phase [22]. For longer holding times ($t \geq 1800$ s), additional peaks are detected, revealing in particular the presence of Be_2Zr and Zr_2Cu crystals [22,24,25]. One can note that the icosahedral phase is still present after 3600 s, as confirmed by the high resolution TEM observation coupled with its Fourier transform shown in figure 7ab, where the typical five field symmetry of I-structure can be observed.

[Insert figure 6 here: XRD spectra after various maintains at 683K]

[Insert figure 7a here: High resolution TEM observation of a crystallite after a holding time of 3600 s at 683 K]

[Insert figure 7b here: Associated Fast Fourier Transform showing an icosahedral structure of the crystallite after a holding time of 3600 s at 683 K]

4.1.2. Volume fraction of crystallites. In order to achieve a quantitative analysis of the reinforcement induced by the presence of nanocrystallites in the studied metallic glass, it is necessary to measure as accurately as possible the volume fraction of nanocrystals. Usually, this fraction is calculated by differential scanning calorimetry analyses [7,26,27] according to:

$$f_v = \int_0^t H(t)dt / \int_0^\infty H(t)dt \quad (1)$$

where $H(t)$ is the released heat flux. This equation assumes that the enthalpy of crystallization does not change with the degree of crystallization and that only one kind of crystals dominates the crystallization process. It also assumes that the alloy is fully crystallized at the end of the transformation, those assumptions being often experimentally not satisfied.

Other techniques like for instance density or resistivity measurements can be used but they require to know associated characteristics of the crystallites, which are frequently unknown [28]. One fruitful way to obtain information about the volume fraction of crystallites in partially crystallized metallic glasses is based on the integrated intensity of the X-ray diffraction pattern, as shown by Wesseling *et al.* [29]. This technique of quantification was performed in the present investigation and despite the small size of the crystallites, the deduced values were validated by a comparison with the values derived from TEM dark field observations of the partially crystallized samples [30]. The corresponding values of the volume fraction f_v of crystals are given in table 1 for the XRD patterns of figure 6 and for an annealing time of 7200 s at 646 K.

[Insert table 1 here: Variation of crystal volume fraction calculated thanks to the XRD patterns with maintains time at 683 K and for 7200s at 646 K (errors are due to the area calculation in the XRD patterns)]

4.1.3. Effect of deformation on crystallization? Before analyzing the various causes of the viscosity increase during deformation, one must wonder about the effect of deformation on crystallization since, as already mentioned, such effects have been reported for various BMGs. Figure 8 displays XRD patterns of samples heat treated for 3600 s at 683 K, one under

1 deformation carried out at $5 \times 10^{-4} \text{ s}^{-1}$ and the other one in static conditions (i.e. no deformation).
2 The two patterns are very similar with the same main peaks, suggesting no detectable effect of
3 deformation on the nature of the crystallites. Moreover, the calculated volume fraction of
4 crystallites corresponding to these XRD patterns show no significant differences since in both
5 cases, a value of $f_v \approx 0.45$ is measured. This value is in agreement with the DSC scans (at 10
6 K/min) shown in figure 9. These scans correspond to four samples heat treated at 683 K for two
7 durations (1800 s and 2500 s), in both static (i.e. no deformation) and dynamic (deformed at a
8 strain rate of $5 \times 10^{-4} \text{ s}^{-1}$) conditions. For the two durations, the curves associated with static and
9 dynamic conditions appear quite similar: two peaks are systematically detected. The first peak
10 corresponds to the remaining of the second crystallization event in the amorphous sample and
11 the second one is due to the third crystallization peak in the amorphous sample. Some
12 differences in the peak temperatures can be nevertheless detected for the samples annealed 1800
13 s. One can also note a slight difference between static and dynamic conditions in the remaining
14 crystallization energy of the first remaining peak. For the two studied durations, the remaining
15 energy of the non deformed sample is a little bit smaller suggesting that strain slightly reduces
16 the crystallization kinetics. In the present study, the loss of the thermal stability of the glass is
17 associated with the production of quasi-crystals. Since quasi-crystallization is expected to be
18 promoted by the presence of an icosahedral short range order (ISRO), if viscous flow increases
19 structural disorder, it may hinder this quasi-crystallization. Such effect has been previously
20 reported in the case of $\text{Zr}_{65}\text{Al}_{7.5}\text{Ni}_{10}\text{Cu}_{12.5}\text{Pd}_5$ BMG deformed by compression in the SLR [16].
21 These analyses support the idea that deformation in the investigated experimental domain has
22 only a marginal effect on crystallization in the studied alloy. It also confirms the results (figure
23 2c and 3) that stress (or viscosity) level after a given time appears to be controlled by the total
24 spent time at the temperature of deformation and not by the strain level.

25 [Insert figure 8 here: XRD spectra of two samples deformed and undeformed
26 during 3600 s at 683 K]

27 [Insert figure 9 here: DSC scans of samples deformed at $5 \times 10^{-4} \text{ s}^{-1}$ and
28 undeformed at 683K during respectively 1800 s and 2500 s]

29 **4.3. Reinforcement effects due to partial crystallization**

30
31 Various mechanical models can be used to predict the reinforcement effect resulting from
32 the increase of particle volume fraction in a viscous medium. However, these models generally
33 require hypotheses related to the characteristics of both the particles and the matrix. Concerning
34 particles, rounded shapes and rigidity are frequently assumed. In the present study, TEM
35 observations of partially crystallized samples before and after large strains ($\epsilon \approx 1.5$) at high
36 temperature did not reveal any significant change in the morphology of the crystallites [30]. This
37 suggests consequently that the crystallites can be considered as rigid particles for the studied
38 conditions of deformation. Moreover, as previously mentioned, quite spherical crystallites are
39 also observed by TEM. Concerning the matrix, it is generally assumed that its characteristics do
40 not vary when the volume fraction of particles increases. In the present case, since the change in
41 particle volume fraction results from crystallization processes, it is of prime importance to get
42 information about a possible change of the composition of the residual amorphous phase. Indeed,
43 such a change can contribute to harden the alloy. For instance, if T_g increases because of a
44 change in the composition, it will induce a decrease of the ratio T/T_g at the given temperature of
45 deformation. A change of the glass transition temperature can be associated to a progressive
46 solute enrichment of the residual amorphous phase during crystallization. Some authors have
47 suggested that beryllium could be rejected from the growing crystals in Vit1 [25,31], since
48 beryllium enrichment tends to increase T_g in ZrTiCuNiBe BMG [32]. In the present
49 investigation, as illustrated by the DSC curves (figures 4a and 4b), only very slight increases of
50

T_g were measured after maintains at 646 K or 683 K, typically less than 3 or 4 K. One must however indicate that for long maintains at 683 K (typically longer than 1800 s, measuring T_g was no longer possible. If the measured apparent activation energy Q_{app} of the Newtonian viscosity for the amorphous alloy is taken into account, such a change of T_g would result in a reinforcement coefficient of about 1.3. It means that this matrix effect remains limited for the studied metallic glass in the selected conditions of deformation.

These comments suggest that simple mechanical models can be reasonably used to predict the reinforcement effect resulting from partial crystallization of the studied BMG. The simplest one is probably the Einstein relationship for which the reinforcement factor R associated to a composite with a crystal volume fraction f_v is given by:

$$R = \frac{\sigma}{\sigma_0} = (1 + 2.5f_v) \quad (2)$$

with σ the flow stress of the composite and σ_0 the flow stress corresponding to the as-provided glass. This relationship has been frequently used in the case of partially crystallized BMGs [10,14]. However, relation (2) leads to very limited reinforcement effect compared to those measured experimentally in this work. For instance, a reinforcement coefficient less than 1.5 is predicted by relation (2) when $f_v \approx 0.15$. Such a volume fraction of crystallites is roughly measured after 7200 s of maintain at 646 K (either in static conditions or during continuous straining) and results in a reinforcement factor close to 7. Similar conclusions can be also drawn for other values of f_v . Therefore the Einstein's relationship is probably not adapted to account for the reinforcement due to crystallization in the studied metallic glass, even for relatively small values of f_v (typically $f_v < 0.2$).

A more general (but less simple) relationship to describe the mechanical behavior of a suspension of particles in a viscous matrix, is given by [33,34], noting that for small crystal volume fraction, this equation is equal to the Einstein's relationship:

$$R = \left[1 - \frac{\phi_v^{eff}}{\phi_v^{max}} \right]^{-2.5\phi_v^{max}} \quad (3)$$

with ϕ_v^{eff} the effective volume fraction of particles and ϕ_v^{max} the maximum packing fraction. ϕ_v^{max} depends on the size and shape distribution of the particles. In the case of randomly dispersed spherical particles with the same diameter, ϕ_v^{max} corresponds to the random close packing (RCP) value, namely $\phi_v^{max} \approx 0.64$. Since in the present investigation, the crystallites are nearly spherical with a narrow size distribution, this assumption is expected to be satisfied. In the present work, as a first approximation, ϕ_v^{eff} is supposed to be equal to f_v . Under this assumption, figure 10 compares the variation with the crystallite volume fraction of both the experimental reinforcement factor (for testing carried out at 683 K) and the factor predicted by relation (3). Except for $f_v = 0.07$ for which the two values are in relatively good agreement, the experimental reinforcement appears much stronger than the predicted one. For $f_v = 0.32$, the measured reinforcement factor is for instance nearly 90 times greater that what is predicted. One must noted that the simplicity of the model is not the cause for this large discrepancy since, as demonstrated by Wolff et al. [26] in a Mg based BMG, more sophisticated analyses lead to similar discrepancy.

[Insert figure 10 here: Curves represent the reinforcement factor versus the crystallized volume fraction according to the Krieger's model with or without modified matrix around the crystals. A modified matrix layer of 4 nm is assumed in the left case. The filled squares represent the lower bound of the reinforcement factor in Newtonian regime during the compression tests at 683K

with an incubation time of 300 s. Values are given for various annealing times: 600 s, 1200 s, 1800 s and 2700 s]

One must keep in mind that relations (2) and (3) are valid only for matrix displaying a Newtonian rheology (i.e. constant viscosity with various strain rates). One can wonder whether such a rheology still holds as far as the glass crystallizes. In order to get information about the rheology of the partially crystallized alloy, strain rate jump tests were carried out on pre-treated alloys. However, at 683 K, the continuous crystallization does not allow performing strain rate jumps after various annealing times with a constant microstructure. Consequently, only tests at 646 K were carried out. The variation of the apparent viscosity with the strain rate for an alloy pre-treated during 7200 s at 646 K is displayed by figure 11 and compared to the behaviour of the glass in as-provided conditions. The viscosities corresponding to the continuous deformation experiment at this temperature are also shown on figure 11 and suggest again that deformation does not affect significantly crystallization in the present studied conditions. The comparison between the as-provided and the pre-annealed alloy clearly shows that, whereas the behaviour is Newtonian for the as cast sample and for applied strain rates lower than $3 \times 10^{-4} \text{ s}^{-1}$, the viscosity is no longer constant with strain rate when the glass is pre-annealed for 7200 s at 646 K. This change in rheology means that the reinforcement factor which is experimentally measured is probably lower than what would be measured if a Newtonian regime could be preserved despite the crystallization process. In other words, the underestimation of the reinforcement factors predicted by relation (3) compared to the experimental ones is probably even greater than what is displayed by figure 10.

[Insert figure 11 here: Relation between viscosity and strain rate at 646K in compression for the as cast sample and for the samples annealed 7200s at 646K with and without deformation]

Such underestimation of the values predicted by relation (3) compared to the experimental reinforcement factors can be related to the hypothesis $\phi_v^{eff} = f_v$. For instance, it is known that geometrical percolation of particles can occur for particle volume fraction close to 0.16 in the case of spherical particles with the same diameter and randomly distributed in a given matrix. However, such a geometrical percolation does not systematically induce a “mechanical” percolation. Indeed, in order to get a “mechanical” percolation, interfacial bonds between the particles are needed and the effect on the mechanical behavior of the composites will be directly related to the strength of the interfaces. In the present investigation, if a geometrical percolation cannot be excluded (despite the fact that crystal clustering is not observed by TEM), it is not expected to result in a significant “mechanical” percolation because crystallites appear spherical and without well established grain- (or phase-) boundaries between them. Moreover, if a skeleton of crystallites is assumed, it is expected to induce apparent strain softening in the first strain steps resulting from its breakdown. Such behaviors were not observed for the partially crystallized samples in the studied experimental conditions as shown in figure 2c and 3.

ϕ_v^{eff} may also differ from f_v if some volumes of matrix are triggered in particle agglomerates or if the matrix in the direct vicinity of the particles displays specific mechanical properties. Such concepts have been already pointed out in the case of particles agglomerates considering that the matrix which is triggered in such agglomerates cannot contribute efficiently to the macroscopic strain [34]. Changes in mechanical behavior of the glass located at the vicinity of the particles have been already reported to explain the unusual reinforcement observed for polymers reinforced by nanoparticles [35,36]. For such nanocomposites, it has been suggested that the macromolecular chains which are anchored on the particle surface could have a reduced mobility compared to the bulk matrix [37], an effect which can be huge in the case of nanometric particles. If a similar hypothesis is considered in the present work, the experimental

reinforcements can be described by relation (3) as illustrated by figure 10, which displays also the predicted reinforcement under the assumption of a thickness of non-deformable matrix around each nanocrystal equal to 4 nm. This curve supports the idea that such effect could account for the reinforcement observed in the partially crystallized BMG even if the origin of such an effect in metallic glasses remains an open question.

5. Conclusion

The interactions between deformation and crystallization were investigated in a bulk metallic glass (Vit1). In the studied conditions, it is shown that the effect of crystallization on the flow stress at high temperature depends mainly on the time spent at the given temperature without significant strain effect. The crystallization was studied by different techniques and the volume fraction of crystals was measured using the XRD patterns for various heat treatments. According to a cross analysis of data, we conclude that the deformation does not change significantly the volume fraction of crystal, the crystal composition neither the crystal size.

The crystallization (in static or dynamic annealing) leads to a strong reinforcement effect which cannot be explained by a dispersion of rigid particles in an amorphous matrix. Additional reinforcement possible origins were discussed: change in residual glass, contribution of the crystals to deformation, connection between particles and nanometer crystallites size effect were proposed. It finally seems that this effect is mainly due to the nanometric size of the crystals and could be taken into account by introducing a non deformable amorphous layer around each crystallite.

Acknowledgements

The authors acknowledge Dr. A. Mussi for his help in some thin foils preparation and TEM observations.

References

- [1] Z. F. Zhang, J. Eckert, L. Schultz, *Acta Mater.*, **51** 1167 (2003).
- [2] J.P Chu, C.L. Chiang, T. Mahalingam, T.G. Nieh, *Scripta Mater.*, **49** 435 (2003).
- [3] K. S. Lee, T.K. Ha, S. Ahn, Y.W.Chang, *J. Non-cryst. Solids*, **317** 193 (2003).
- [4] Y. Kawamura, T. Nakamura, H. Kato, H. Mano, A. Inoue, *Mat. Sci. Eng. A*, **304-306** 674 (2001).
- [5] M. Bletry, P. Guyot, Y. Brechet, J.J. Blandin, J.L. Soubeyroux, *Mater. Sci. Eng. A* **387-389** 1005 (2004)
- [6] J. Lu, G. Ravichandran, W.L. Johnson, *Acta Mater.*, **51** 3429 (2003).
- [7] C. Fan, D. V. Louzguine, C. Li, A. Inoue, *Appl. Phys. Lett.*, **75** 340 (1999).
- [8] A. Inoue, *Intermetallics*, **8** 455 (2000).
- [9] J. Basu, N. Nagendra, Y. Li, U. Ramamurty, *Phil. Mag.*, **83** 1747 (2003).
- [10] T. A. Waniuk, R. Busch, A. Masuhr, W. L. Johnson, *Acta Mater.*, **15** 5229 (1998).
- [11] W.J. Kim, *Intermetallics*, **15** 282 (2007)
- [12] S. Puech, J.J. Blandin, J.L. Soubeyroux, *Advanced Engineering Materials*, **9** 764 (2007)
- [13] W.J. Kim, D.S. Ma, H.G. Jeong, *Scripta Mater.*, **49** 1067 (2003).
- [14] T. G. Nieh, J. Wadsworth, C. T. Liu, T. Ohkubo, Y. Hirotsu, *Acta Mater.*, **49** 2887 (2001).
- [15] B. Gun, K.J. Laws, M. Ferry, *J. of non-crystalline solids*, **352** 3887 (2006)

Formatted: Font: Bold

Formatted: Font: Bold

Formatted: Font: Bold

- 1
2 [16] J. Saida, S. Ishihara, H. Kato, A. Inoue, H.S. Chen, Appl. Phys. Lett., **80** 4708
3 (2002).
4 [17] A. Masuhr, T.A. Waniuk, R. busch, W.L. Johnson, Phys. Rev. Lett., **82** 2290
5 (1999).
6 [18] D. Suh, R.H. Dauskardt, J. Mater. Res., **17** 1254 (2002).
7 [19] M. Bletry, P. Guyot, Y. Brechet, J.J. Blandin, J.L. Soubeyroux, Acta Mat., **54**
8 1257-1263 (2006).
9 [20] H. Kato, Y. Kawamura, A. Inoue, H.S. Chen, Appl. Phys. Lett., **73** 3665 (1998).
10 [21] A. Reger-Leonhard, M. Heilmaier, J. Eckert, Scripta Mater., **43** 49 (2000).
11 [22] X.-P. Tang, J.F. Löffler, W.L. Johnson, Y. Wu, J. Non-Cryst. Solids, **317** 118
12 (2003).
13 [23] J.F. Löffler, W.L. Johnson, Appl. Phys. Lett., **76** 3394 (2000).
14 [24] R.C.Y. Tam, C.H. Shek, Mater. Sc. Eng. A, **364** 198 (2004).
15 [25] I. Martin, T. Ohkubo, M. Ohnuma, B. Deconihout, K. Hono, Acta Mater., **52** 4427
16 (2004).
17 [26] U. Wolff, N. Pryds, E. Johnson, J.A. Wert, Acta Mater., **52** 1989 (2004).
18 [27] Z. Bian, G. He, G.L. Chen, Scripta Mater., **46** 407 (2002).
19 [28] K.L. Sahoo, A.K. Panda, S. Das, V. Rao, Mater. Lett., **58** 316 (2004).
20 [29] P. Wesseling, B.C. Ko, J.J. Lewandowski, Scripta Mater., **48** 1537 (2003).
21 [30] S. Gravier, PhD Thesis, Institut National Polytechnique de Grenoble (2006)
22 [31] J.M. Pelletier, B. Van de Moortèle, J. Non-Cryst. Solids, **325** 133 (2003).
23 [32] W.H. Wang, H.Y. Bai, J. Appl. Phys., **84** 5961 (1998).
24 [33] I.M. Krieger, Adv. Coll. Interf. Sc., **3** 111 (1972).
25 [34] D. Quemada, Eur. Phys Journal, AP **1** 119-227 (1998).
26 [35] E. Chabert, R. Dendievel, C. Gauthier, J.Y. Cavallé, Comp. Sc. Tech. **64** 309
27 (2004).
28 [36] G.M. Odegard, T.C. Clancy, T.S. Gates, Polymer, **46** 553 (2005).
29 [37] P.G. De Gennes, 'La matière ultradivisée' in 'L'ordre du chaos', Ed. Bibliothèque
30 pour la science, (1989), p. 128-135.
31
32
33
34
35
36
37
38
39
40
41
42
43
44
45
46
47
48
49
50
51
52
53
54
55
56
57
58
59
60

TABLE

Temperature (K)	683				646
Annealing time (s)	600	1200	1800	2700	7200
f_v	0.07 ± 0.03	0.17 ± 0.03	0.27 ± 0.03	0.32 ± 0.03	0.16 ± 0.04

Table I

Variation of crystal volume fraction calculated thanks to the XRD patterns with maintains time at 683 K and for 7200s at 646 K (errors are due to the area calculation in the XRD patterns).

For Peer Review Only

FIGURES

Figure 1: Viscosity vs. strain rate in compression for the amorphous alloy at various temperatures

Figure 2a: Flow stress vs. strain at 646 K for various strain rates

Figure 2b: Apparent viscosity vs. time at 646 K for various strain rates

Figure 2c: Reinforcement factor vs. time curves at 646 K and $1.5 \times 10^{-4} \text{ s}^{-1}$ for various incubation times at 646 K: 300 s, 3600 s and 7200 s

Figure 3: Reinforcement factor vs. time curves at 683 K and $5 \times 10^{-4} \text{ s}^{-1}$ for various incubation times at 683 K: 300 s, 900 s, 1500 s and 2050 s

Figure 4a: DSC curves at a heating rate of 10K/mn of the as cast sample, and of samples annealed 1800 s and 7200 s at 646K.

Figure 4b: DSC curves at a heating rate of 10K/mn of the as cast sample, and of samples annealed 1200 s and 3600 s at 683 K.

Figure 5a: Bright field TEM observations of a sample heat treated at 683 K for 600 s

Figure 5b: Bright field TEM observations of a sample heat treated at 683 K for 2700 s

Figure 5c: Dark Field TEM observation of a sample annealed 7200 s at 646 K

Figure 6: XRD spectra after various holding times at 683K.

Figure 7a: High resolution TEM observation of a crystallite after a holding time of 3600 s at 683 K

Figure 7b: Associated Fast Fourier Transform showing an icosahedral structure of the crystallite after a holding time of 3600 s at 683 K

Figure 8: XRD spectra of two samples deformed and undeformed during 3600 s at 683 K

Figure 9: DSC scans of samples deformed at a strain rate of $5 \times 10^{-4} \text{ s}^{-1}$ and undeformed at 683K during respectively 1800 s and 2500 s

Figure 10: Curves representing the reinforcement factor versus the crystallized volume fraction according to the Krieger's model with or without modified matrix around the crystals. A modified matrix layer of 4 nm is assumed in the left case.

The filled squares represent the lower bound of the reinforcement factor in Newtonian regime during the compression tests at 683K with an incubation time of 300s. Values are given for various annealing times: 600s, 1200s, 1800s and 2700s.

Figure 11: Relation between viscosity and strain rate at 646K in compression for the as cast sample and for the samples annealed 7200s at 646K with and without deformation.

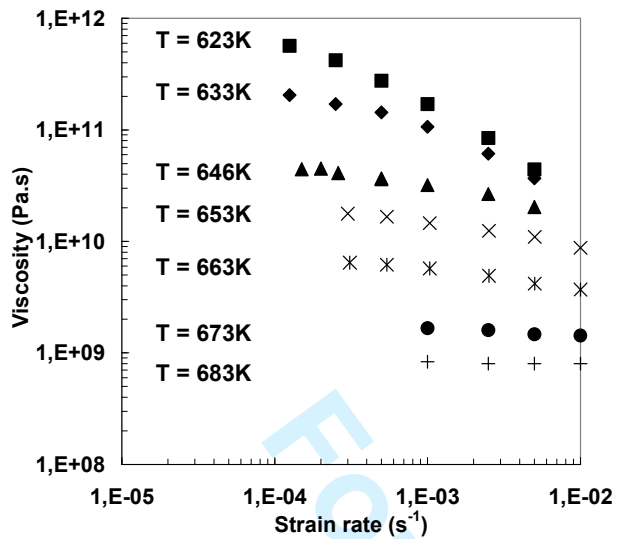


Figure 1

Viscosity vs. strain rate in compression for the amorphous alloy at various temperatures

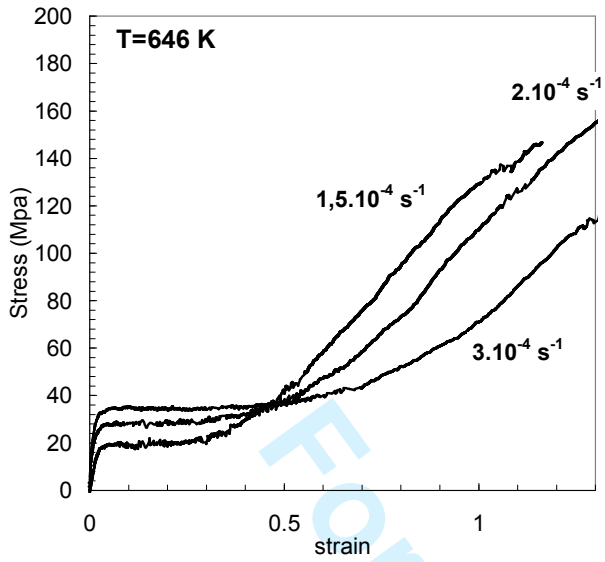


Figure 2-a :
Flow stress vs. strain at 646 K for various strain rates

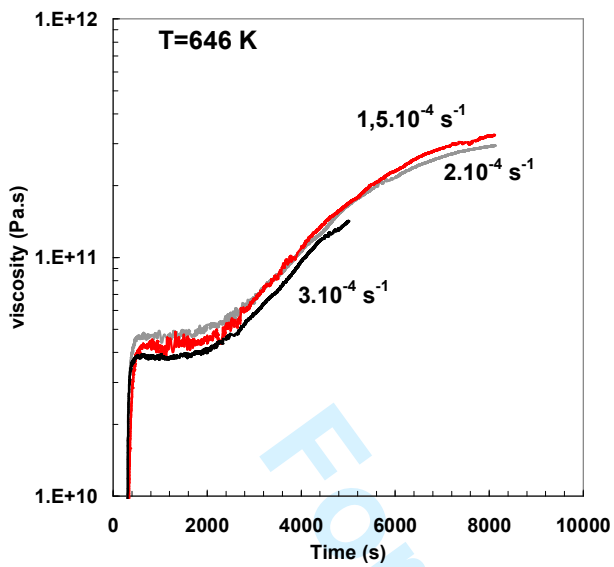


Figure 2b :
Apparent viscosity vs. time at 646 K for various strain rates

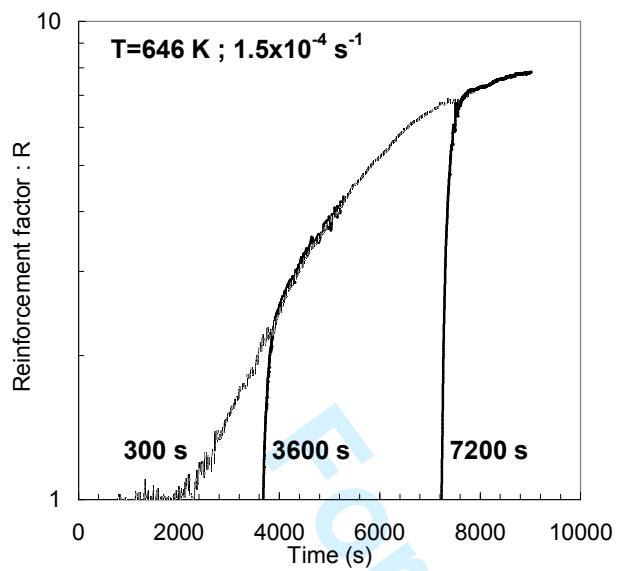


Figure 2c:
Reinforcement factor vs. time curves at 646 K and $1.5 \times 10^{-4} \text{ s}^{-1}$ for various incubation times at 646 K: 300 s, 3600 s and 7200 s

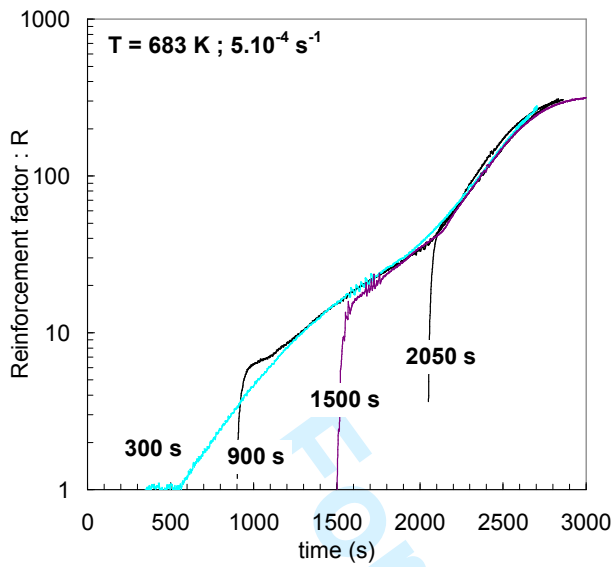
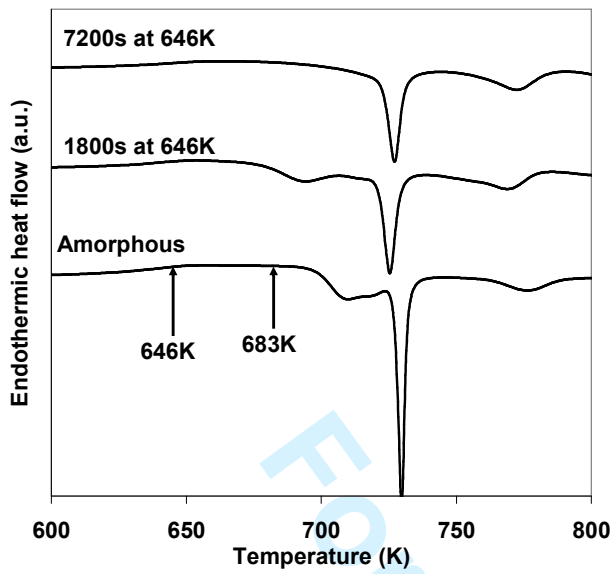


Figure 3
Reinforcement factor vs. time curves at 683 K and $5 \times 10^{-4} \text{ s}^{-1}$ for various incubation times at 683 K: 300 s, 900 s, 1500 s and 2050 s

**Figure 4a**

DSC curves at a heating rate of 10K/mn for the as cast sample, and for samples annealed 1800 s and 7200 s at 646K.

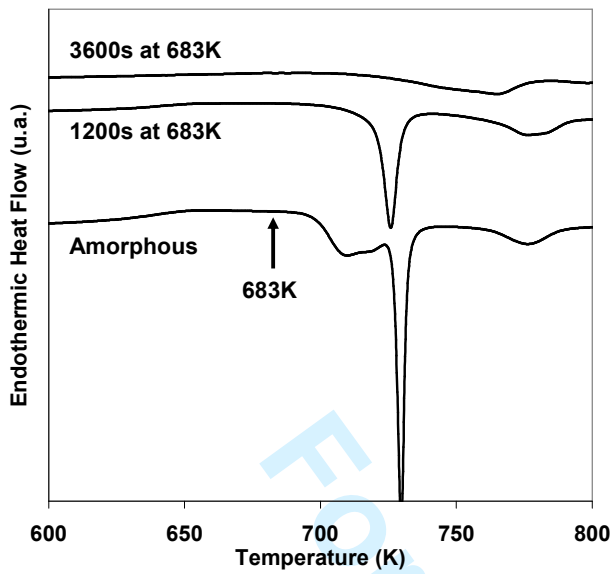


Figure 4b

DSC curves at a heating rate of 10K/mn of the as cast sample, and of samples annealed 1200 s and 3600 s at 683 K.

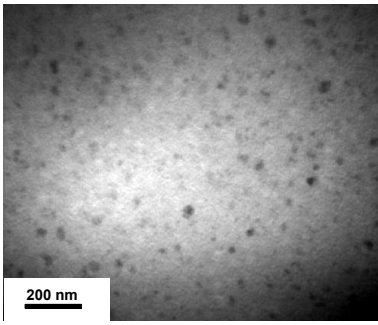
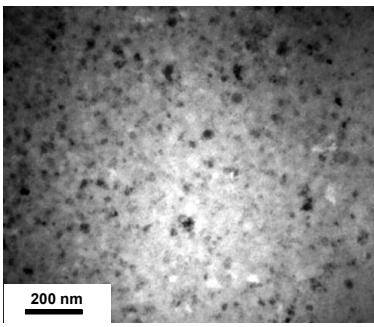


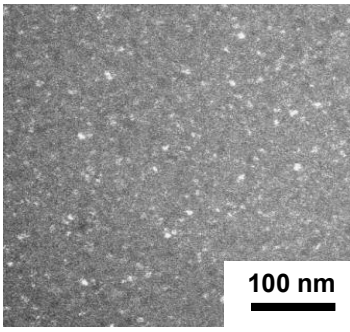
Figure 5a:
Bright field TEM observations of a sample heat treated at 683 K for 600 s

For Peer Review Only



13 **Figure 5b:**
14 Bright field TEM observations of a sample heat treated at 683 K for 2700 s
15
16
17
18
19
20
21
22
23
24
25
26
27
28
29
30
31
32
33
34
35
36
37
38
39
40
41
42
43
44
45
46
47
48
49
50
51
52
53
54
55
56
57
58
59
60

For Peer Review Only



13
14 **Figure 5c:**
15 Dark Field TEM observation of a sample annealed 7200 s at 646 K
16

17
18
19
20
21
22
23
24
25
26
27
28
29
30
31
32
33
34
35
36
37
38
39
40
41
42
43
44
45
46
47
48
49
50
51
52
53
54
55
56
57
58
59
60

For Peer Review Only

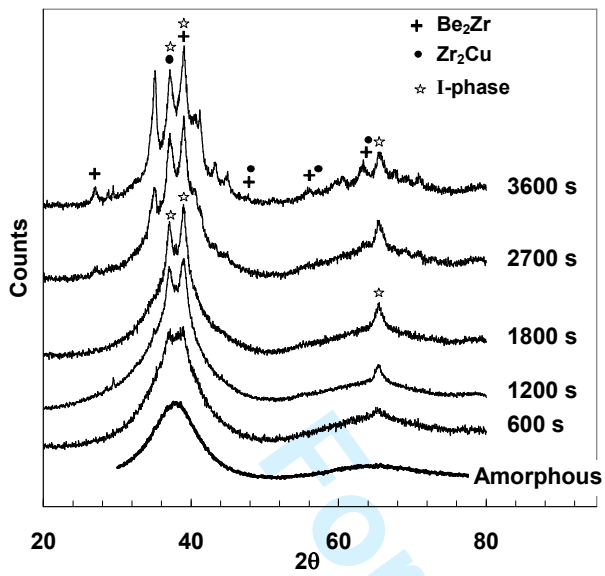


Figure 6
XRD spectra after various holding times at 683K.

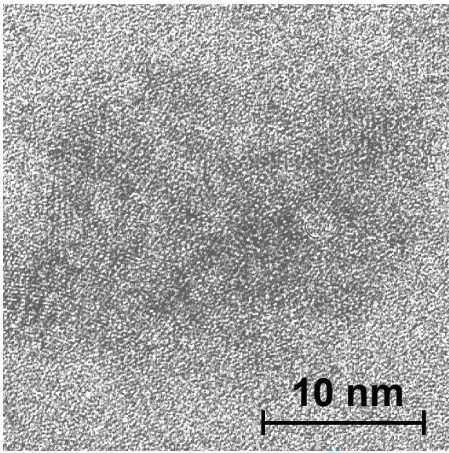


Figure 7a

High resolution TEM observation of a crystallite after a holding time of 3600 s at 683 K

Open Peer Review Only

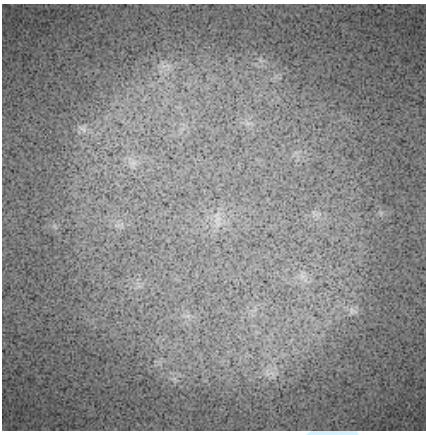


Figure 7b: Associated Fast Fourier Transform showing an icosahedral structure of the crystallite after a holding time of 3600 s at 683 K

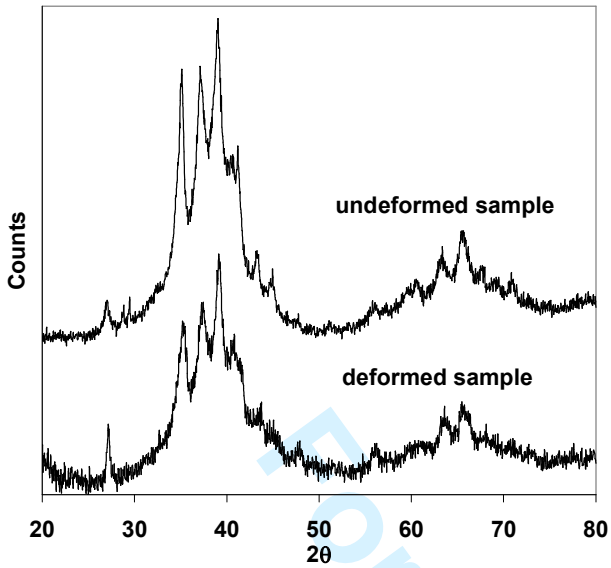


Figure 8
XRD spectra of two samples deformed and undeformed during 3600 s at 683 K

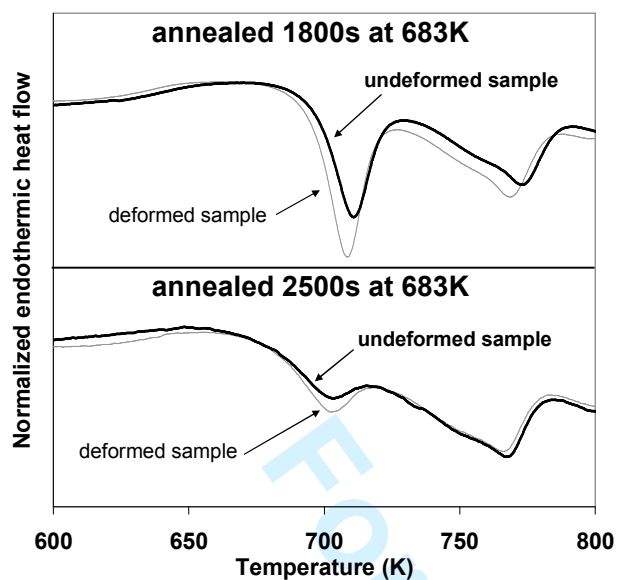


Figure 9
DSC scans of samples deformed at a strain rate of $5 \times 10^{-4} \text{ s}^{-1}$ and undeformed at 683K during respectively 1800 s and 2500 s

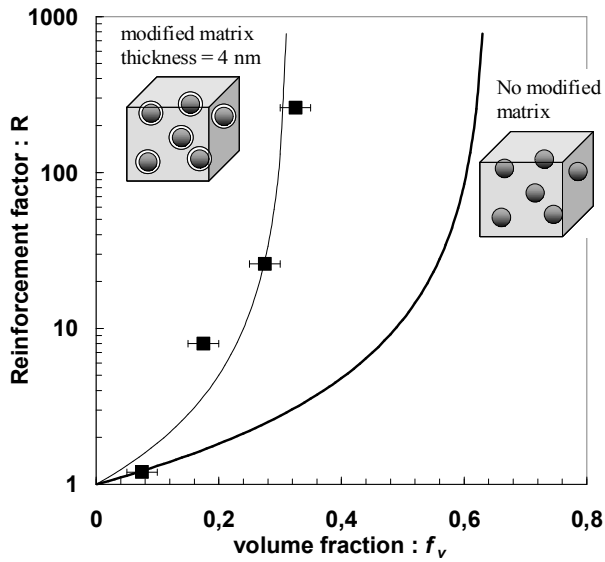


Figure 10

Curves represent the reinforcement factor versus the crystallized volume fraction according to the Krieger's model with or without modified matrix around the crystals. A modified matrix layer of 4 nm is assumed in the left case.

The filled squares represent the lower bound of the reinforcement factor in Newtonian regime during the compression tests at 683K with an incubation time of 300s. Values are given for various annealing times: 600s, 1200s, 1800s and 2700s.

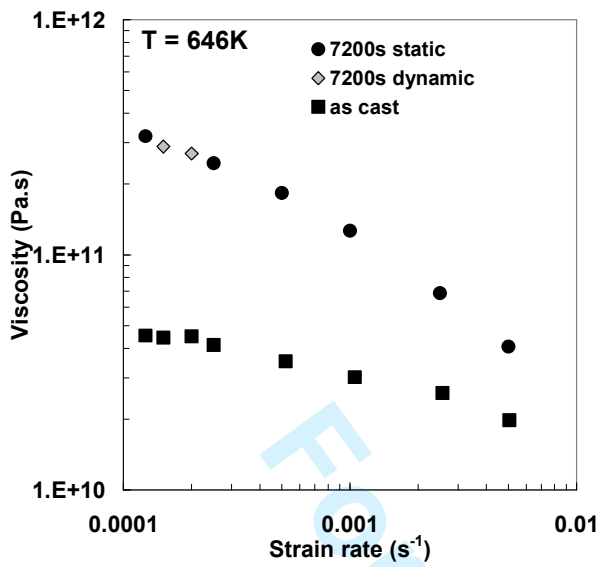


Figure 11

Relation between viscosity and strain rate at 646K in compression for the as cast sample and for the samples annealed 7200s at 646K with deformation (dynamic) and without deformation (static).